Article

Not peer-reviewed version

LaserFit: A Low-Cost Laser-Based Optical Power Meter for Cycling

Gennady Lubarsky *

Posted Date: 12 May 2026

doi: 10.20944/preprints202605.0740.v1

Keywords: fitness and activity tracking; biomechanics instrumentation; position-sensitive detectors; laser diodes; embedded systems

 doi:10.20944/preprints202605.0740.v1

Article

LaserFit: A Low-Cost Laser-Based Optical Power Meter for Cycling

Gennady Lubarsky [1,2]

[1] Laser Spoke Limited, Carrickfergus, BT38 7UN, UK; g.lubarsky@ulster.ac.uk or gena.lubarsky@gmail.com

[2] The School of Engineering, Ulster University, Belfast, UK

Abstract

Cycling is one of the most popular sports and recreational activities. Millions of new people start to integrate bicycling into their daily routines every year. Fitness and activity trackers are the most powerful motivation tools for cycling novices and serious cycling enthusiasts. For this purpose, we present LaserFit, a laser-based direct force power meter for fitness and activity tracking during cycling. We developed embedded hardware to collect the torque and the wheel rotation data, which is produced by a laser-based position sensing system mounted on the rear wheel to precisely record the power output produced by the rider during cycling. The sensor data transmits to a smartphone via Bluetooth/ANT+ for data acquisition and analysis. Our device can be produced at low costs and deliver a level of accuracy similar to that obtained with the most expensive systems available on the market. To evaluate the accuracy of our system extensive experiments were conducted. The results of the present study suggest that the LaserFit power meter provides a strong relationship (r = 0.97) across a range of trials in laboratory and field conditions when compared with the SRM power meter. The LaserFit is therefore considered a valid alternative for training and performance measurement during continuous cycling.

Keywords: fitness and activity tracking; biomechanics instrumentation; position-sensitive detectors; laser diodes; embedded systems

1. Introduction

Cycling is one of the most efficient and popular ways to control weight and commute. Active transport represents a potentially powerful way to meet the recommended levels of physical activity for many populations, it offers a great potential to improve health and has several other positive side effects: it is non-polluting, poses little danger to others, and is socially inclusive [1–4]. Self-efficacy and motivation are crucial to people's engagement with cycling, either leisure, commuting or road racing. Fitness and activity trackers are promoted on the basis that data analysis, combined with encouragement to maintain or improve personal states of fitness, will empower wearers to adopt positive health habits [5]. The fitness wearable industry is booming and increasingly popular, with an estimated 19 million connected wearables purchased in 2014 compared to 5.9 million in 2013 and asubstantial increase by 2020 [6]. There are many off-the-shelf solutions, such as Fitbit, Garmin, Polar, Apple Watch, etc., to measure calorie expenditure during walking and running. However, monitoring calories spent while riding a bike or track of cyclist activity and fitness are not straightforward tasks. To accurately estimate caloric expenditure, cyclists have to install a bike computer or use a smartphone connected to additional torque sensors mounted on their bikes. Currently, the typical solution is using a cycling power meter [7]. In modern training programs, this device is the ultimate tool routinely used by professional coaches to examine the performance of elite-level cyclists. However, these peripherals are costly, complicated and inconvenient for daily use. This paper addresses the need for an accurate, universal, user-friendly and affordable power measurement device for cyclists.

 doi:10.20944/preprints202605.0740.v1

To address this challenge, we propose an optical system to detect, record and transmit information about the cyclist's efforts during riding. The system is mainly composed of two components: (i) an Embedded optical hardware system installed on the rear wheel and (ii) PC and smartphone applications.

The present research seeks to overcome the problems associated with the prior art by providing a torque monitoring apparatus and giving an improved power meter which is universal and allows monitoring of power output produced by riders of different types of human-powered vehicles. Further objectives provide an improved power meter which is simple and inexpensive to use and manufacture; which is universal, transferable and can be mounted on most common types of bicycles and tandems; which is based on a contactless method; which is accurate and reliable; and which measures actual power output.

The article is organised as follows. Section II surveys existing methods for energy expenditure and power monitoring systems for cyclists. We present the system architecture of LaserFit in Section III and explain the core algorithms in Section IV. Experimental evaluation is given in Section V. Discussion & Future Work are presented in Section VI and Section VII concludes the article.

2. Background and Related Work

Power output has been described as the most direct measure of the rider's efforts during cycling despite its higher variation compared with heart rate [7,8]. Portable power meters are devices that can be installed on a bicycle to measure cyclists' power output in the field. The detailed data obtained from power meters are used to monitor and evaluate cyclists' training and race performances [9].

The cyclist's power can be measured using a device known as a power meter, which often relies on the pedal-torque, crank arm torque or wheel torque measurements. Due to recent technological developments, bicycle power meters are becoming part of the training equipment of professional cyclists and are used by cyclists to improve their training [10]. The cyclist's power mainly depends on the torque. The torque generated by a cyclist during the wheel rotation is the most critical performance index for cyclists because the cyclist's power output can provide precise and accurate measurements of the cyclist's performance and fitness. Neither speed nor heart rate alone can provide the same precision as direct power measurement for quantifying cycling performance. Speed depends on the road grade, wind velocity, terrain, and the athlete's physical characteristics, such as muscle and heart rate, which are controlled by the athlete's current health, diet, and fatigue [11].

To monitor the power, one needs to equip the bike with a portable system able to acquire, calculate and display data throughout the riding process. In the late 1980s, portable power meters became commercially available, enabling the direct measurement of power. After more than three decades of development, a wide range of devices for measuring dynamic parameters in bicycles has been proposed. These devices have been implemented successfully on all moving parts of the bicycle propulsion system, starting from the crank through the chain to the rear hub. Power meters are operating in various ways, but utilise a similar physical principle: measuring the force applied to one of the moving elements of the power delivery system and the element velocity caused by this force. Force can be measured in power metering systems directly or indirectly - as a momentum produced by this force - a torque. An ideal power meter should not be in contact with the propulsion system to avoid any inaccuracy in the power measurements, a. In practice, the power converted to the vehicle motion is not equal to the power produced by the human body due to energy loss in transmission elements. The measurement should be performed as close to the power output as possible to measure the actual power available. For example, in bicycles, the power output is at the point of contact between the rear wheel tire and the ground. This property is also essential for power meters used on tandems - vehicles driven by more than one cyclist.

Torque measurements are typically performed using strain gauges fixed to the pedals, the crank, and the chain wheel. Power meters were first developed in the 1980s with SRM (Schoberer Rad Messtechnik, Welldorf, Germany) generally being acknowledged as the first to produce a commercially available system. A patent to Schoberer [12] discloses a power meter with deformation

 doi:10.20944/preprints202605.0740.v1

elements built into the chainring. The deformation of the element is measured by strain gauges and the angular velocity is calculated from the counting of the crank rotation. Acquired data were used to calculate the torque created on the crank. However, to install this power meter, an existing chainring needs to be removed. This power meter is produced from precise mechanical parts and as a result, is expensive and not transferable from bike to bike.

Another method to measure power on bicycles is proposed by Gerlitzski [13]. An optical sensor is placed on the bottom bracket and used to measure the distance the pedal spindle twists and the angular velocity of the spindle is measured several times per crank revolution. This power meter requires the replacement of the bottom bracket with the specially designed one. Due to the specifics of construction, the device can be used to measure the power input from the left leg only. A power meter based on the direct measurement of the force exerted in a drive chain is proposed by Cote et al. [14]. The system includes chain vibration and velocity sensors. The frequency of vibration is translated to the chain tension and used with the value of its velocity to calculate the power output. The accuracy of this method is very dependent on the correct system installation, which is not straightforward and needs to be performed by skilled personnel. Another power meter based on direct force measurements is disclosed by Wyatt [15]. The device uses a flexible force sensor inserted in a cycling shoe to record the force applied by the cyclist to the pedal. This data is used in an approximate mathematical model of cycling to calculate an averaging power input from a cyclist's foot. This does not measure the propulsion system. A power metering system based on the monitoring of the rear wheel twisting is described by Mercat [16]. The angular divergence between the hub and the rim created by torque is detected using a disk and a hoop attached to the hub and the rim respectively. Openings formed in the disk and the hoop pass in front of photosensitive detectors. The signal produced by both detectors is used to compute the torque. The method essentially consists in measuring the angular displacement of a peripheral region of the wheel about its central region. Since on a majority of bicycles this displacement is very small, the signal-to-noise ratio produced by this device is low. To install this power meter to a bicycle requires the mounting of a large and specifically built hoop and disk. The installation must be done by a reasonably skilled mechanic with specific tools for the job.

New smartphone apps and opposing force power meter systems have been developed over the last several years to provide cyclists with many of the same power meter features but at a fraction of the cost and complexity.

With the advancements in smartphone GPS sensors, the determination of cyclist power output can now be calculated using speed, cadence, elevation gain and opposing wind speeds, all without the need to affix strain gauge power meters to bicycle components [17–19].

New opposing force power meter systems [20] calculate the power using both opposing forces as well as external speed and cadence sensors for determining an inferred power output. Unlike the SRM power meter that uses up to 20 different strain gauges, these systems only use sensors to measure road gradient, opposing wind forces, barometric pressure and accelerations.

These indirect power measurement approaches considered "power estimation" are not always accurate and unable to resolve rapid changes in speed, riding and wind directions [21] and as a result may produce significant errors.

3. LaserFit Principle of Operation

Figure 1a shows forces distribution operating in the bicycle propulsion system during riding. The rider applies force F_P to the pedals to propel the bicycle. It produces the traction force F_T in the contact between the rear wheel and the ground to overcome a sum of aerodynamic, inertia, resistance and gravitational forces operating along the longitudinal direction F_R.

 doi:10.20944/preprints202605.0740.v1

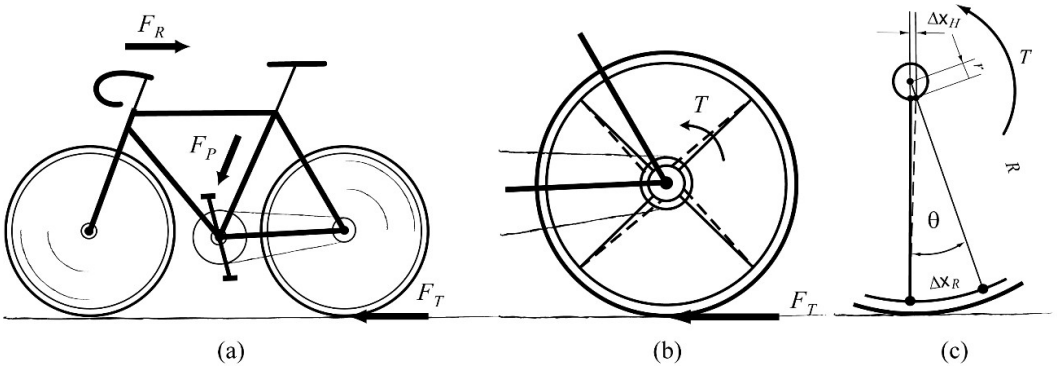

Figure 1. Illustration of a typical bicycle in operation. (a) Main forces operating in a propulsion system; (b) a rear wheel of the bicycle with applied torque; (c) a fragmentary side view of a rear wheel and its deformation.

Force F_P transmits, with finite efficiency, to the rear wheel through the bicycle drivetrain system: from pedals to the front sprocket, to the chain, and the rear sprocket. Depending on the type of lubrication, vehicle age, the gear ratio and cycling regime, the efficiency of typical bicycle transmissions may vary from 85 to 99% and may be as low as 75% in an old bike with rusty parts. Therefore, measuring power performed on the rear wheel is more accurate and provides information on the actual power output produced by the system.

As shown in Figure 1b the rear sprocket is fixedly secured to the hub of the rear wheel. Torque T created on the hub transfers to the contact area between the rear wheel and the ground by the set of spokes, a rim, and a tire. The rear wheel has a certain level of flexibility and operates as a torsion spring twisting proportionally to the applied torque. As deformations of the hub, the rim, and the tire are very small due to their construction and rigidity, the twisting mainly occurs in the spokes region (dashed lines in Figure 1b). This process is illustrated in more detail in Figure 1c. The torque T applied to the hub bends the spokes and causes angular displacement of the hub about the rim. The angle of the twist θ is expressed as:

$$\theta = \frac{T}{k} \tag{1}$$

where k is the torsion elastic modulus of the wheel. This coefficient is mainly depending on the wheel construction, materials, and the bicycle setup. The torsion modulus can be obtained experimentally for any wheel from a simple calibration procedure, which will be described later in this text. Depending on the applied torque and properties of the wheel, the angle of the twist is usually between 0.1 and 1 degree. The angular displacement of the hub can be expressed as:

$$\Delta x_H = r \tan\theta = r \tan\frac{T}{k} \tag{2}$$

where r is a radius of the hub. On the majority of modern bicycles, this dimension is about 15-20mm. It is easy to assume that the angular displacement produced on the hub is very small and not of practical use. However, if one considers this imaginary line projected to the rim (Figure 1c) this produces a much greater shift due to the enlarged distance:

$$\Delta x_R = (r + R) \tan\theta = (r + R) \tan\frac{T}{k} \tag{3}$$

where R is the distance between the hub and the rim surfaces. This dimension varies for many wheels from 250 to 300mm making Δx_R shift large enough for practical measurements.

Thus, for rotating wheels, power can be derived as:

$$P = T\omega \tag{4}$$

where ω is the angular velocity of the wheel. Combining this equation with the expression for the shift yields the power output of the wheel:

 doi:10.20944/preprints202605.0740.v1

$$P = \omega k \tan^{-1} \frac{\Delta x_R}{r + R} \quad (5)$$

Thus, for a wheel with known geometry, the power output can be calculated from measurements of the shift Δx_H and the angular velocity.

Practically, the shift Δx_H can be detected with a laser-based optical system as illustrated in Figure 2. A laser module and a one-dimensional position-sensitive detector (1D-PSD) are permanently attached to the hub of the rear wheel and a right-angle optical prism is attached to the rim. The prism is used as a retro-reflecting device to redirect the beam at 180 degrees. The laser beam deflection detected by the sensor in this arrangement doubled due to the extended travelling length of the laser beam $2R$.

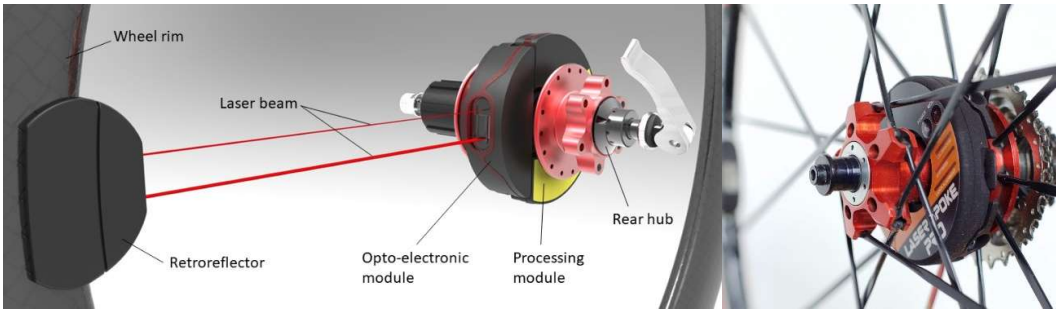

(**a**) (**b**)

Figure 2. Laser-based fitness and activity sensor for cyclists. (a) Schematic diagram of optical system installed on the rear wheel (spokes not shown); (b) Photo of the experimental prototype used for testing.

In operation, the optical system rotates together with the wheel and a coherent and parallel beam is continuously projected from the laser module, reflected by the prism and forms a light spot on the detector surface. The slight axial rotation of the rim relative to the hub caused by pedalling torque moves the relative positions of the prism and detector. As a result, the position the light enters and then exits the prism shifted, although the return direction of the reflected light is not. The sensor, in turn, produces an electrical signal, which is proportional to the position of the light spot, the beam deflection and the applied torque. If the wheel is not loaded, the signal is equal to zero or has a minimal value. Simply put, our method enables using the bicycle wheel as a torsional spring to measure applied torque. This system can be installed on any bicycle, allowing power output measurement on racing and recreational bicycles as well as on BMXs, MTB, fixed bikes, and tandems.

The angular velocity of the wheel was detected by measuring centripetal acceleration with accelerometers.

The power can be calculated using equation 5 if the wheel geometry is well defined, and the wheel torsion coefficient is known. This coefficient can be obtained from the wheel calibration as described below.

4. System Architecture

LaserFit is composed of an optoelectronic unit attached to the hub of the driving bicycle wheel, as shown in Figure 2. The unit functions are data acquisition, pre-processing and transmission via a wireless connection. Also, an application running on the personal computer provides the users with a basic wheel setup and options to download training session data. The rest of this section presents the hardware design of the embedded system unit and the PC application.

4.1. Optical System

In an optical system, shown in Figure 2(a), a beam of light from a collimated semiconductor laser situated on the hub of the bicycle wheel projects on to retro-reflector prism attached to the rim. The light from the laser reflected in the hub where it was focussed by a cylindrical lens onto PSD. In the

 doi:10.20944/preprints202605.0740.v1

optical module printed circuit board, as shown in Figure 3(a) the laser and the sensor have been placed at a precise separation distance. The distance was between the laser axis and the electrical centre of PSD.

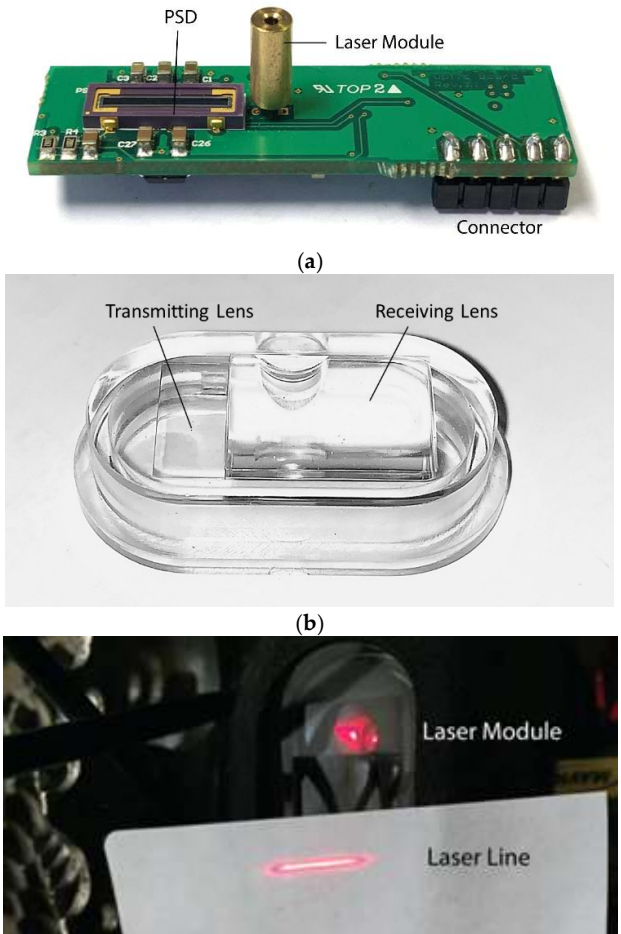

Figure 3. Elements of LaserFit optical system. (a) Optical printed circuit board populated with a laser module and position sensitive detector. (b) An integrated lens. (c) Laser line image at distance 300mm from source.

The optical performance of the design was analysed using Zemax optical simulation software. This traces rays from the laser through the transmit side of the hub optic out to the prism and back through the hub focusing optic to the detector. Analysing one million rays leaving the laser and their subsequent position on the detector plane allows us to calculate the focus quality and optical efficiency. By moving the optical components, it is possible to determine how sensitive the design is to angular and positional tolerances.

4.2. Lenses and Prism

The detector window was covered with a cylindrical lens to improve the laser beam stability, alignment and focusing; and to provide additional protection to the optical components. The lens design, which combines both the transmit and receive optical surfaces, is shown in Figure 3(b). The receiving lens form is a conic curve with a radius of curvature of 15.0mm and a conic constant of -3.72. The centre thickness is 3.735mm. The distance between the back surface of the lens and the top of the detector window is 12.2mm.

 doi:10.20944/preprints202605.0740.v1

The prism design is a simple right-angle prism with an entrance aperture size of 18.4mm x 12.6mm. The prism has been installed in a slightly tilting position to avoid any problems with a ghost reflection from the front face. In operation, the prism shift moves the position at which the light enters the cylindrical lens, which causes the image to move on the detector. The movement of the image, shown in Figure 3(c), is measured by the detector. From this position shift, the torque applied to the wheel can be calculated, which with a measurement of the speed of rotation allows a calculation of rider power output to be made.

4.3. Position Sensitive Detector

As continuous position sensors, PSDs are unparalleled. Compared with discrete element detectors, such as the charge-coupled device (CCD) sensor, the PSD features nanometer positioning resolution, sub-microsecond response times, simple interface circuits, and high reliability.

In this study one-dimensional PSD S3932 (Hamamatsu Photonics, Japan) [22] has been used. This sensor has a photosensitive area of 1 × 12 mm and is mounted on a compact ceramic package with a transparent resin window. The device consists of a uniform resistive layer formed on one surface of a high-resistivity semiconductor substrate, and a pair of electrodes formed on both ends of the resistive layer for extracting the position signal. The active area, which is also a resistive layer, has a PN junction that generates photocurrent using the photovoltaic effect.

To limit the noise level, the distance between the PSD and pre-amps was reduced. The two-channel 16-bit ADC was well bypassed and located near the gain stage amps as shown in Figure 4.

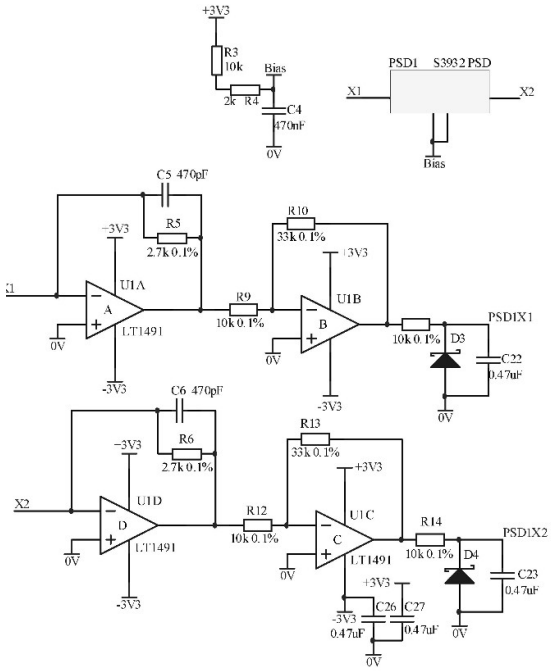

Figure 4. The 1-D optical position sensor uses two op-amps in each leg of the PSD. The first stage is located near the PSD, and the voltage generated is negative with respect to ground. The second stage inverts the signal from the pre-amp stage back to a positive voltage for the 16-bit ADC located on the main board.

Our circuit is laid out on two PCBs with the power coming from a lithium polymer battery mounted underneath the mainboard. The battery drives an efficient charge-pump regulator and voltage inverter for operating the rail-to-rail op-amps Linear Technology LT1491 [23]. All of the op-amps use 0.1% precision resistors, as these tolerances are required for measurement accuracy; the rest of the component tolerances are standard. The instrument is designed to operate with a laser module of 1 mW of power and a PSD wavelength responsivity of 0.40 A/W.

 doi:10.20944/preprints202605.0740.v1

When a spot of light strikes the sensor surface, an electric charge proportional to the light intensity is generated at the incident position. This charge is driven through the resistive layer and collected by the output electrodes as photocurrents I_1 and I_2 while being divided in inverse proportion to the distance between the light spot position and each electrode. The relation between the incident light position and the photocurrents from the output electrodes is given by

$$\frac{I_2 - I_1}{I_1 + I_2} = \frac{2x}{L} \tag{6}$$

where x is the distance from the electrical centre of PSD and L is the length of the active area.

The position resolution of a PSD is the minimum detectable displacement of a spot of light on the detector's surface; it is dependent on detector area, light intensity, bandwidth, and temperature. In our application, PSD operates at a low frequency. This application uses low bandwidth, relatively high intensity, and low noise to give a good resolution.

4.4. Hardware Boards

Our embedded system consists of a microcontroller, a laser module, a one-dimensional position-sensitive photodetector (PSD), a two-channel, 16-bit A/D converter, Bluetooth/ANT+ module and on-board memory for data storage. For this study, we decided to design PCBs because it makes development much easier. We used a small pre-amp optical PCB for the position-sensitive detector and the laser module shown in Figure 4; and the larger one for the rest of the circuitry as shown in Figure 5.

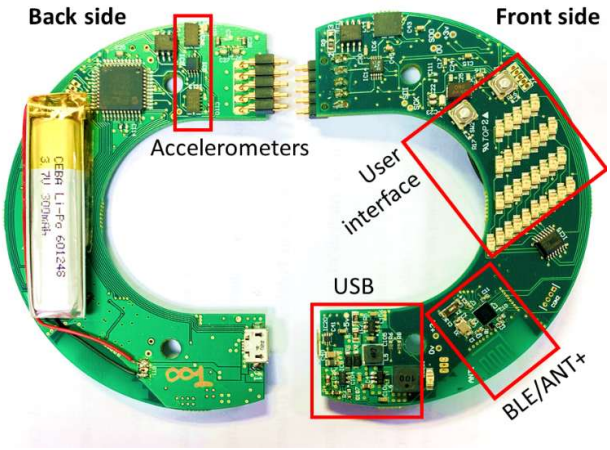

Figure 5. The main board.

The main hardware board, shown in Figure 5, is designed for data pre-processing, storage and transmission. The PCB also accommodates accelerometers, a basic user interface; and a USB circuit for lithium polymer battery charging and serial communication.

The signal generated by the PSD is amplified and filtered for better signal quality. Then the analogue signals are converted to digital signals for later steps. The adopted AD converter is LTC1865 [24] with a sampling rate of 8000Hz and 16-bit resolution. The ADCs were well bypassed and located near the gain stage amps.

The digital signals are then sent to a micro-controller via the I2C interface. Displacement signals are stored in built-in memory for later processing. The adopted micro-controller is the high-performance STM32F105RC [25], which is widely used in consumer electronic products and portable medical equipment.

The data frames are sent to a Bluetooth/ANT+ module through UART and further sent to the smartphone by the Bluetooth module with an SPP profile at a data rate of 150 KBit/s. Bluetooth ensures reliable wireless data transmission within a distance of 10m, which is adequate for our system. A rechargeable LiPo battery is adapted to power the whole hardware board.

 doi:10.20944/preprints202605.0740.v1

The power output is stored in the computational unit and displayed to the rider by a radio transceiver.

4.5. Firmware and Software

The firmware for this device is written in C. The main task is interrupt-driven by the timer. It continually acquires data from the two-channel ADC and accelerometers, solves the position and the angular velocity equations, and then stores the data and sends it to BLE/AN+ module for transmission. The Mode and Power push buttons are polled to determine if the user has pressed them.

We wanted the PSD to be able to produce good results without the use of an optical filter even under extremely intense ambient light. Thus, the firmware implements a first-order infinite impulse response (IIR) low-pass filter [26,27].

LaserFit incorporates two wireless communication protocols: ANT+ and Bluetooth. The firmware incorporates Bluetooth Cycling Power Generic Attribute (GATT) profile [28], and the system operates as a Cycling Power Sensor. This approach offers true two-way communication and uploads data captured during training on cycling computers, smartphones and watches already on the market. ANT+ [29] is another gold standard for over-the-air communication in the cycling and athletic industries. The system is simple, robust, and well-accepted thanks to the proliferation of Garmin's GPS display units. ANT+ bike power data format implemented using a simple Power-Only message transmitted at a slow rate along with more detailed main power messages at a higher data rate. ANT+ antenna provides for those riders looking to add power to their ANT+ devices, whether from Garmin or another manufacturer. Thus, there was no need to develop any LaserFit-specific mobile application as the end-user can choose from many applications available for cyclists and analyse their training with different online services. Instead, we developed a utility PC software (Figure 6) with a range of basic functions giving the user options to configure the system: the wheel stiffness and circumference, sampling rate as well as to download the training sessions.

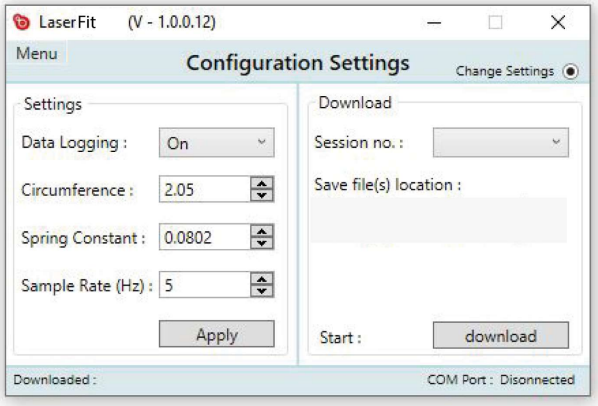

Figure 6. LaserFit software user interface.

5. Testing

5.1. Wheel Stiffness Calibration

The tangential stiffness of wheels is a complex function of multiple variables: sizes, tension, geometries and number of spokes. It also depends on wheel construction, and materials and varies for different manufacturers and models. The behaviour of bicycle wheels subjected to tangential loads may be accurately modelled by idealising the system [29]. For real-life applications, however, a direct calibration is required to find a relationship between the deformation of the wheel and the torque applied to the wheel.

 doi:10.20944/preprints202605.0740.v1

With the LaserFit power meter installed on the wheel, the calibration process is straightforward. For calibration, the rim of the wheel was fixed and known torque was applied to the hub. The torque was applied using a specially designed lever with a defined length and integrated with a chain whip. Static calibration is performed by suspending known variable weights on the end of the lever. The laser beam deflections corresponding to the torque were recorded. Figure 7 shows the reaction of the wheel to the applied torque. This initial test demonstrates an excellent wheel response, which is proportional to the force applied to the lever. The plot shows that the laser beam is at zero position when there is no load and returns to zero position after the load removal.

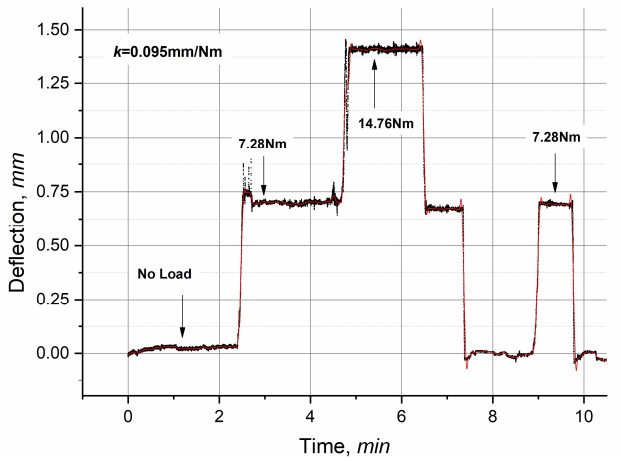

Figure 7. Initial test of the wheel deformation under applied loads.

Two rear wheels Mavic Cosmic and Ksirium (Mavic SAS, Annecy, France) were calibrated in our lab. These wheels are chosen as they present very different mechanical construction and performance - Cosmic is a high-performance wheel designed with a 40mm carbon rim. At the same time, Ksirium is a very popular budget wheel featuring an aluminium rim and bladed spokes. The calibration process has been conducted with known weights (dependent variable) suspended in the lever varying from 5 to 85N with increment steps of 5N. Then, the coefficient of torsion was calculated by the fitting the data to the equation

$$k = \frac{x}{T_C} \tag{7}$$

where T_C is a calibration torque and x is the deformation of the wheel. Calibration results are presented in Figure 8. Both wheels demonstrate a linear response to the load - when the suspending weight increases during the calibration process, the deformation output voltage also increases linearly. The calibration was performed in a range from zero to 35Nm. This range is sufficient to determine a mathematical relationship between the produced torque and the output deformation. Therefore, an approximate linear fit line is plotted through data points for determining the relationship between torque and the deformation as in Equation 7. This mathematical equation is utilised to measure the generated torque on the wheel during cycling when the cyclist is on track. Also, the mathematical equation may be used to measure the generated torque out of the calibration range. Results of our test show that the Cosmic wheel outperforms the Ksirium wheel as it is 8% stiffer in a tangential direction.

5.2. In Laboratory Testing

All tests were conducted on a road bike (Pinarello Dogma, Cicli Pinarello SRL, Italy) with a frame size of 56 cm. The bike was equipped with an SRM Science Road power meter comprising 20 strain gauges (Schoberer Rad Messtechnik, Juelich, Germany) and was used as the reference device. The ability of this device to precisely measure power to within 0.5% of error makes it a gold standard in

 doi:10.20944/preprints202605.0740.v1

the industry [30–35]. The SRM power meter was calibrated before the study according to the methods of Wooles, et al. [36] to assure accurate measures. Calibrated Mavic Cosmic wheel was installed on the bike and used in testing. LaserFit system was fitted to the wheel hub and the prism was attached to the rim.

During the laboratory tests, the bike was mounted on CycleOps PowerBeam Pro trainer (Saris Cycling Group Inc., USA) that operated as an additional power meter with controlled resistance.

Power output was collected simultaneously from three systems using a portable, standalone WASP-N unit (North Pole Engineering, Inc., Minneapolis, USA). This unit provides a bridge for ANT+ devices to communicate wirelessly through Wi-Fi networks to other devices. In our setup WASP received data from three systems via ANT+ channels and translated the data into Wi-Fi packets captured on a smartphone using the WASP Utility application. Data were sampled at 1 Hz throughout the testing. The recorded data were downloaded from the smartphone and further analysed using publicly available software (Golden Cheetah, version 3.5). Figure 8 shows an example line graph comparing the three different power meters measuring power output in watts (y-axis) and time (x-axis) for a 10-minutes workout. The figure shows a steady-state and very good agreement between all three power meters. The LaserFit also has very similar power output characteristics but seemed to show a better response to the sudden load changes, as its power output is following closer to the one from the PowerBeam Pro system.

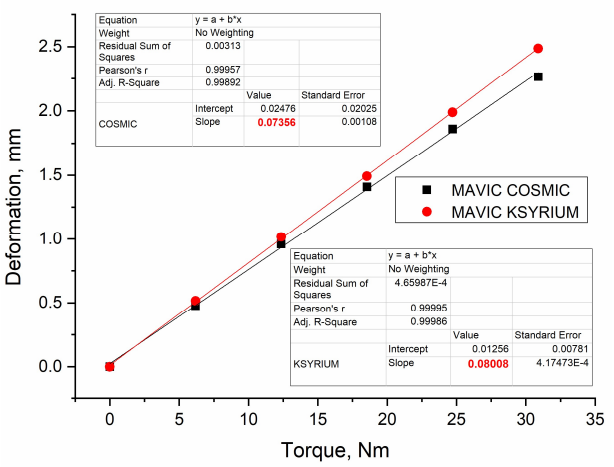

Figure 8. Calibration plots produced for two different wheels.

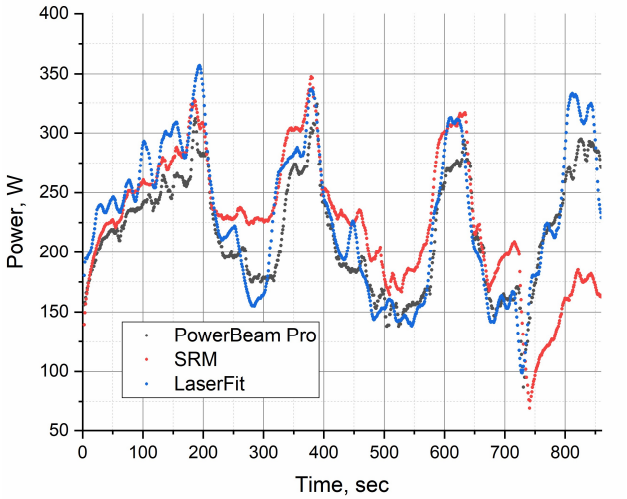

 doi:10.20944/preprints202605.0740.v1

Figure 8. Example power data line graph representing power outputs across three different power meters in lab.

5.3. Field Testing

In the field test, the same bike equipped with an SRM power meter and fitted with the LaserFit system has been used. The rider performed for an hour-long ride that consisted of both city and road riding. Figure 9 shows how well the two power meters compared to each other. The figure demonstrates the linear fit of two power outputs and R-values (Pearson's correlation coefficient) produced when comparing the two power meters. When fitted across all corresponding points, the line slope was 0.98. Also, the r-value determines the linear relationship (strength) between the two power meters, with R-values of 0.97 having a near-perfect relationship.

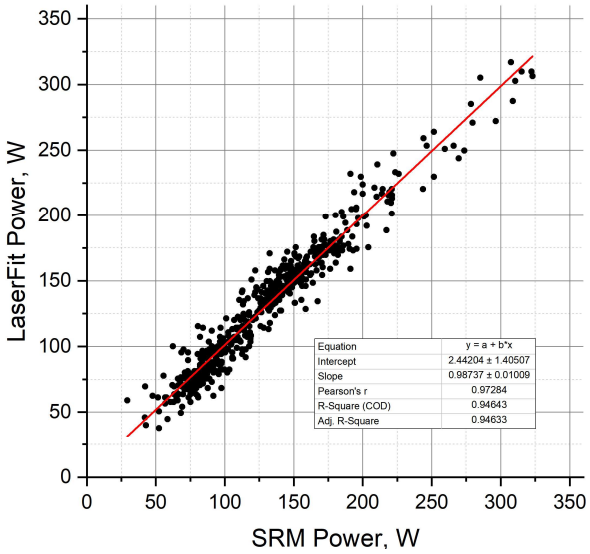

Figure 9. Correlations of power output between the SRM and the LaserFit device in the field test.

6. Discussion and Future Work

From the experimental results, we can see that LaserFit has high performance in power output and torque monitoring while riding the bike. These advantages enable us to provide trustable suggestions on activity and fitness tracking during cycling.

A major reason for the good performance is the high-precision laser-based system adopted by LaserFit.

The one-dimensional position-sensitive detector guarantees high-quality signal samplings by effectively reducing the ambient light noise. LaserFit utilises an optical method to track cyclist efforts by monitoring the deformation of the rear wheel available on any bike. This allows our systems to work on any bicycle, enabling their use on racing and recreational bicycles as well as on BMXs and tandems.

The health benefits of practising aerobic, endurance sports such as cycling provide the essential purpose that is at the root of nearly everybody's motivation. LaserFit now can be used as a powerful motivational tool to promote cycling by providing an easy and affordable way of tracking activity and fitness while riding a bike. It can help end-users to set up their personal goals and analyse the progress of performance. LaserFit can be used as an accurate calorie-burned calculator, helping commuters and recreational cyclists to integrate cycling into their everyday healthy routine. For serious cycling enthusiasts, LaserFit is a precise power meter that delivers a level of accuracy similar to that obtained with the most expensive systems available on the market. As a direct force power meter, it measures the actual torque produced to propel the bike. By measuring forces at the end of

 doi:10.20944/preprints202605.0740.v1

the propulsion system - the spokes region, LaserFit monitors an actual power output available for competition. It shows an integrated performance of the rider and the bike and may also be used as a method to assess the wheel performance and tuning.

In the future, we plan to improve LaserFit in several aspects further. First, experiments in this study are conducted in a lab and field environment with low light conditions; bright sunlight was reduced as much as possible. The position sensing processing will be improved with ambient light suppression by using the advanced position-sensitive detector to allow any level of environmental light and still maintain the same level of accuracy as the current version of LaserFit.

Second, the user interface will be improved and integrated with the smartphone utility application to streamline the setup and interaction with the device. Third, we also plan to add new capabilities to LaserFit, such as identifying the cadence and gears, estimating the user performance precisely, and riding style and help to improve the cycling experience. Last but not least, we intend to reduce further the overall size of the optical module and the embedded system unit to optimise installation and improve mechanical performance. The specific target is to design an embedded system unit without a USB socket, which can be wirelessly charged and controlled by the utility app. All these improvements will be validated in long-term real-life settings.

7. Conclusions

Accurate and affordable power measurement remains a key challenge for the growing cycling community. Existing power meters are either expensive, difficult to install, or limited to specific bicycle configurations. There is a clear need for a universal, low-cost solution that measures actual power output at the wheel.

In this paper, we have presented LaserFit, a laser-based direct force power meter for fitness and activity tracking during cycling. The developed system is a functional wireless force platform capable of measuring the forces acting on the wheel during real cycling usage. We developed embedded hardware to collect the torque and the wheel rotation data, which is produced by a laser-based position sensing system mounted on the rear wheel to precisely record the power output produced by the rider during cycling. The sensor data is then sent to a smartphone via Bluetooth/ANT+ for data acquisition and analysis.

Extensive experiments are conducted to evaluate the accuracy of our system. The results of the present study suggest that the LaserFit power meter provides a strong relationship ($r = 0.97$) across a range of trials in laboratory and field conditions when compared with the SRM power meter. The LaserFit is therefore considered a valid alternative for training and performance measurement during continuous cycling.

Our device is also distinct in that it can be produced at low costs and deliver a level of accuracy similar to that obtained with the most expensive systems available on the market. Moreover, it may act as an experimental basis for the development of new bicycle components and new studies on the biomechanics of cycling.

Funding: This work was supported in part by the Invest Northern Ireland Research and Development Grant RD0215368.

Data Availability Statement: The original contributions presented in this study are included in the article. Further inquiries can be directed to the corresponding author(s).

Conflicts of Interest: The authors declare no conflict of interest. The funders had no role in the design of the study; in the collection, analyses, or interpretation of data; in the writing of the manuscript, or in the decision to publish the results.

References

1. T. Götschi, J. Garrard, and B. Giles-Corti, "Cycling as a Part of Daily Life: A Review of Health Perspectives," *Transport Reviews,* vol. 36, no. 1, pp. 45-71, 2016/01/02 2016.

 doi:10.20944/preprints202605.0740.v1

2. B. De Geus and I. Hendriksen, "Cycling for transport, physical activity and health: What about Pedelecs? " 2015.
3. J. Woodcock, P. Banister D Fau - Edwards, A. M. Edwards P Fau - Prentice, I. Prentice Am Fau - Roberts, and I. Roberts, "Energy and transport," (in eng), no. 1474-547X (Electronic).
4. P. Oja et al., "Health benefits of cycling: a systematic review," (in eng), *Scand J Med Sci Sports,* vol. 21, no. 4, pp. 496-509, Aug 2011.
5. C. P. Andrew Hilts, and Jeffrey Knockel. (2016). *Every Step You Fake: A Comparative Analysis of Fitness Tracker Privacy and Security.*Available: https://openeffect.ca/reports/Every_Step_You_Fake.pdf
6. S. Asimakopoulos, G. Asimakopoulos, and F. Spillers, "Motivation and User Engagement in Fitness Tracking: Heuristics for Mobile Healthcare Wearables," *Informatics,* vol. 4, no. 1, p. 5, 2017.
7. H. Allen and A. Coggan, *Training and Racing with a Power Meter, 2nd Ed*. VeloPress, 2015.
8. S. Vogt et al., "Power output during stage racing in professional road cycling," (in eng), *Med Sci Sports Exerc,* vol. 38, no. 1, pp. 147-51, Jan 2006.
9. L. Passfield, J. G. Hopker, S. Jobson, D. Friel, and M. Zabala, "Knowledge is power: Issues of measuring training and performance in cycling," (in eng), *J Sports Sci,* vol. 35, no. 14, pp. 1426-1434, Jul 2017.
10. R. Tielert, N. Wehn, T. Jaitner, and R. Volk, "Power Measurement in Cycling using inductive Coupling of Energy and Data (P80)," 2008.
11. G. E. F. Pawelka, "The innovation equation: balancing clever technical solutions with users' needs," *Procedia Engineering,* vol. 2, no. 2, pp. 2613-2617, 2010/06/01/ 2010.
12. U. SCHOBERER, "POWERMETER FOR A CRANK DRIVE," Germany Patent WO/1989/000401, 1989.
13. G. Siegfried, "Method and device for determining the torque exerted on a rotating body which can be rotationally driven around a rotational axis," USA Patent US6,356,847, 1998.
14. C. J.-J. Cote Alan, Croy John C., Nissila Seppo, "Method and apparatus for measuring power output and for measuring tension and vibrational frequency of an elongate flexible member," USA Patent 6199021, 1998.
15. S. Wyatt Jeffrey, Knapp Richard, "Systems and Methods of Power Output Measurement," USA Patent 11380945, 2009.
16. M. Jean-Pierre, "Method and device for measuring the torque transmitted by the driving wheel of a cycle and a cycle equipped with said device," USA Patent US4811612A, 1986.
17. J. Stragier, M. Vanden Abeele, P. Mechant, and L. De Marez, "Understanding persistence in the use of Online Fitness Communities: Comparing novice and experienced users," *Computers in Human Behavior,* vol. 64, pp. 34-42, 2016/11/01/ 2016.
18. L. R. West, "Strava: challenge yourself to greater heights in physical activity/cycling and running," *British Journal of Sports Medicine,* vol. 49, no. 15, p. 1024, 2015.
19. A. Zhan, M. Chang, Y. Chen, and A. Terzis, "Accurate caloric expenditure of bicyclists using cellphones," presented at the Proceedings of the 10th ACM Conference on Embedded Network Sensor Systems, Toronto, Ontario, Canada, 2012. Available: https://doi.org/10.1145/2426656.2426664
20. P. Merkes Pfj Fau - Menaspà, C. R. Menaspà P Fau - Abbiss, and C. R. Abbiss, "Validity of the Velocomp PowerPod Compared With the Verve Cycling InfoCrank Power Meter," (in eng), no. 1555-0273 (Electronic).
21. T. H. Witte and A. M. Wilson, "Accuracy of non-differential GPS for the determination of speed over ground," *Journal of Biomechanics,* vol. 37, no. 12, pp. 1891-1898, 2004/12/01/ 2004.
22. Hamamatsu Photonics. *One-dimensional PSD S3932*. Available: https://www.hamamatsu.com/jp/en/product/type/S3932/index.html
23. Analog Devices. *AD Homepage: LT1491*. Available: https://www.analog.com/en/products/lt1491.html
24. Analog Devices. *AD Homepage: LTC1865*. Available: https://www.analog.com/en/products/ltc1865l.html
25. STMicroelectronics. *ST Homepage: STM32F105RC*. Available: https://www.st.com/content/st_com/en/products/microcontrollers/stm32-32-bit-arm-cortex-mcus/stm32-mainstream-mcus/stm32f1-series/stm32f105-107/stm32f105rc.html
26. G. D. Halikias and I. M. Jaimoukha, *Design of Infinite Impulse Response (IIR) filter with almost linear phase characteristics*. 2015.
27. R. Johnson and C. Lentz, "2-D optical position sensor," *Circuit Cellar: East Hartford, CT, USA,* pp. 1-7, 2003.

 doi:10.20944/preprints202605.0740.v1

28. BluetoothSIG. (2016, 2020). *Bluetooth SIG ProprietaryCycling Power Profile*. Available: https://www.bluetooth.org/DocMan/handlers/DownloadDoc.ashx?doc_id=412769
29. H. P. Gavin, "Bicycle-Wheel Spoke Patterns and Spoke Fatigue," 1996.
30. P. F. J. Merkes, P. Menaspà, and C. R. Abbiss, "Validity of the Velocomp PowerPod Compared With the Verve Cycling InfoCrank Power Meter," (in eng), *Int J Sports Physiol Perform,* pp. 1-6, Oct 2 2019.
31. G. P. Millet, N. Tronche C Fau - Fuster, D. J. Fuster N Fau - Bentley, R. Bentley Dj Fau - Candau, and R. Candau, "Validity and reliability of the Polar S710 mobile cycling power meter," (in eng), no. 0172-4622 (Print).
32. A. Nimmerichter, L. Schnitzer, B. Prinz, D. Simon, and K. Wirth, "Validity and Reliability of the Garmin Vector Power Meter in Laboratory and Field Cycling," (in eng), no. 1439-3964 (Electronic).
33. A. Nimmerichter, L. Schnitzer, B. Prinz, D. Simon, and K. Wirth, *Validity and Reliability of the Garmin Vector Power Meter in Laboratory and Field Cycling*. 2017.
34. J. G. Pallares and J. R. Lillo-Bevia, "Validity and Reliability of the PowerTap P1 Pedals Power Meter," (in English), *Journal of Sports Science and Medicine,* Article vol. 17, no. 2, pp. 305-311, Jun 2018.
35. J. G. Pallarés and J. R. Lillo-Bevia, "Validity and Reliability of the PowerTap P1 Pedals Power Meter," (in eng), no. 1303-2968 (Electronic).
36. A. L. Wooles, A. J. Robinson, and P. S. Keen, "A static method for obtaining a calibration factor for SRM bicycle power cranks," *Sports Engineering,* vol. 8, no. 3, pp. 137-144, 2005/01/01 2005.